

## Studies on Electroplated Copper Indium Telluride Thin Films

T.Mahalingam<sup>1,\*</sup>, S.Thanikaikarasan<sup>1</sup>, C.Sanjeeviraja<sup>1</sup>, Taekyu Kim<sup>2</sup>, P.J.Sebastian<sup>3</sup> and Yong Deak Kim<sup>4</sup>

<sup>1</sup>Department of Physics, Alagappa University, Karaikudi-630 003, India.

<sup>2</sup>Centre for Modeling and Simulation Studies, Security Management Institute, Kangnam-Ku, Seoul- 135 731, Republic of Korea

<sup>3</sup>Solar Hydrogen Fuel Cell Group, Energy Research Centre, UNAM, 62580, Temixco, Morelos, Mexico.

<sup>4</sup>Department of Electrical and Computer Engineering, Ajou University, Suwon-443 749. Republic of Korea.

Received: July 29, 2009, Accepted: August 4, 2009

**Abstract:** Thin films of copper indium telluride were electrodeposited on indium doped tin oxide coated conducting glass (ITO) substrates at various bath temperatures and deposition potentials from an aqueous acidic bath containing  $\text{CuSO}_4$ ,  $\text{In}_2(\text{SO}_4)_3$  and  $\text{TeO}_2$ . The deposited films were characterized by x-ray diffraction, scanning electron microscopy, energy dispersive analysis of x-rays and optical absorption techniques, respectively. The film structure was found to be cubic with preferential orientation along (200) plane. Using x-ray diffraction data the microstructural parameters such as crystallite size, strain, dislocation density and stacking fault probability were calculated. The variation of microstructural parameters with bath temperature and deposition potential were studied. The experimental observations are discussed in detail.

**Keywords:** thin films,  $\text{CuInTe}_2$ , x-ray diffraction, microstructural parameters, optical properties, surface morphology.

### 1. INTRODUCTION

Thin films of chalcopyrites find numerous applications in a variety of solid state devices such as visible and infrared light emitting diodes, solar cells, IR detectors and photovoltaic devices [1-6]. Among them, copper indium telluride ( $\text{CuInTe}_2$ ) is a direct band gap semiconductor with a band gap value in the range between 0.92 and 1.06 eV which make them quite interesting for solar energy conversion [7]. Polycrystalline thin films of  $\text{CuInTe}_2$  are usually crystallized in cubic structure (PDF-89-2380) with lattice constant ( $a=6.080 \text{ \AA}$ ) and in the tetragonal structure (PDF-81-1937) with lattice constants ( $a= 6.194 \text{ \AA}$ ;  $c= 12.415 \text{ \AA}$ ). There are several techniques reported for the preparation and characterization of  $\text{CuInTe}_2$  crystals and thin films. Some examples are: Bridgmann method [7], co-evaporation technique [5], thermal evaporation [8]. Electrodeposition and chemical bath deposition are the alternative methods that are particularly adapted for the preparation of chalcogenide materials. Chemical deposition of chalcogenides are already used for producing interfacial layers in high efficiency thin film solar cells. The chalcopyrite compounds have been the objects of numerous studies concerning thin film deposition from aqueous solution. Recently, electrodeposition has now emerged as a simple, economical and viable technique to

synthesize good quality films for device applications. The attractive features of this method are: low cost synthesis, low temperature growth, convenience for producing large area devices and the possibility to control the film thickness and morphology by readily adjusting the electrical parameters as well as the composition of the electrolytic solution [9, 10]. Structural, morphological, compositional and electrical properties of In rich  $\text{CuInTe}_2$  thin films prepared using electrodeposition technique were investigated by Orts et al [11]. Ishizaki et al have prepared  $\text{CuInTe}_2$  thin film from an acidic bath by electrodeposition and studied their structure, morphology, composition and optical properties [1]. All the research workers have dealt with the determination of structure type and qualitative observation of defects and grain size of  $\text{CuInTe}_2$  thin films. No quantitative measurements were made on the microstructural parameters of electrodeposited  $\text{CuInTe}_2$  thin films. The microstructural parameters such as crystallite size, strain, dislocation density and stacking fault probability are found to influence the physico chemical properties of electrodeposited  $\text{CuInTe}_2$  thin films. In addition to this, the reduction of stress, dislocation density and increase in crystallite size of  $\text{CuInTe}_2$  thin films may be useful for opto-electronic applications. To our knowledge, no report is available concerning the microstructural parameter evaluation of electrodeposited  $\text{CuInTe}_2$  thin films.

\*To whom correspondence should be addressed: Email: maha51@rediffmail.com

In the present work, we describe the preparation of  $\text{CuInTe}_2$  thin films on indium doped tin oxide coated conducting glass (ITO) substrates at various bath temperatures and deposition potentials using electrodeposition technique. The microstructural parameters were evaluated and the effect of bath temperature and deposition potential on the above properties of the films were studied. Also, the morphological, compositional and optical, properties of the films are studied and the results are discussed.

## 2. EXPERIMENTAL DETAILS

The electrochemical deposition of  $\text{CuInTe}_2$  thin films on indium doped tin oxide (ITO) coated conducting glass substrates were carried out potentiostatically containing 0.001 M  $\text{CuSO}_4$ , 0.005 M  $\text{In}_2(\text{SO}_4)_3$  and 0.0005 M  $\text{TeO}_2$ . All the electrochemical experiments were carried out in a standard three electrode system using a scanning potentiostat (EG & G, Model 362, Princeton Applied Research, USA) with ITO substrate as working electrode and graphite plate as counter electrode. A saturated calomel electrode was immersed into the bath and kept very nearer to the working electrode. Both working and counter electrodes are brought close to each other to obtain good quality films. The two surfaces facing each other were kept parallel, so that the released ions will be attracted and deposited exactly perpendicular to the cathode surface. During the time of deposition the electrolytic bath was stirred slowly using magnetic stirrer cum heater set up. The plating experiments were carried out at various bath temperatures ranging from 35°C to 80°C with different intervals of time. Series of films were prepared in the potential range between -500 and -1100 mV versus SCE. Smooth, uniform and well adherent films of  $\text{CuInTe}_2$  were obtained under optimized condition.

Thickness of the deposited films was estimated using stylus profilometer (Mitutoyo SJ-301, USA). X-ray diffraction studies was carried out using a (X'Pert PRO PANalytical, Netherlands) x-ray diffractometer with  $\text{CuK}_\alpha$  radiation with  $\lambda=1.5418 \text{ \AA}$ . Optical properties was carried out at normal incidence at room temperature using an UV-Vis-NIR spectrophotometer (HR-2000, M/S Ocean Optics, USA). Surface morphological studies was carried out using a scanning electron microscope (JEOL JSM 840). The film composition was analyzed using an energy dispersive x-ray analysis set up attached with SEM.

## 3. RESULTS AND DISCUSSION

### 3.1. Film thickness

The deposition of  $\text{CuInTe}_2$  thin films was controlled by two independent variables such as (i) film thickness and its uniformity (ii) surface morphology [12]. Thickness of the deposited films was estimated using stylus profilometer. The average thickness of the deposited layers can be directly controlled by controlling the plating current and the plating time. During deposition, it was observed that at higher bath temperature (such as 65°C and above) the film formation is hindered due to hydrogen evolution. At lower bath temperatures (such as below 50°C) an irregular growth with rough surface was obtained. Fig. 1.a,b,c. shows the variation of film thickness with deposition time for films deposited at various bath temperatures from 35 to 65°C. It is observed from Fig. 1 that the film thickness increases linearly with deposition time and tend to attain saturation. The bath temperature is expected to influence the

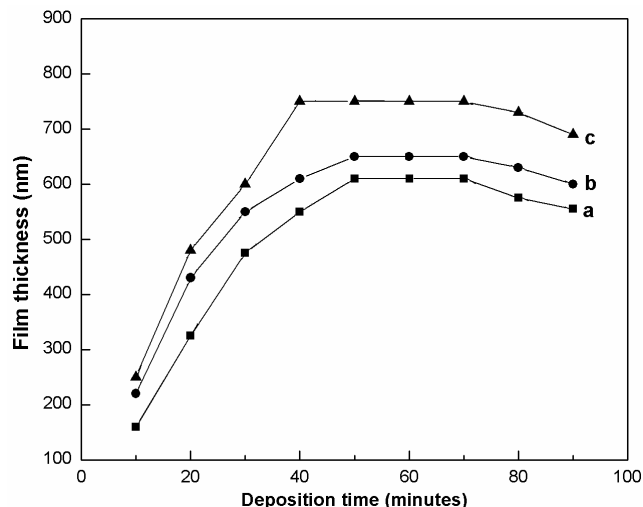


Figure 1. Variation of film thickness with deposition time for  $\text{CuInTe}_2$  thin films electrodeposited at various bath temperatures (a) 35°C, (b) 50°C (c) 65°C.

deposition rate by: (i) increase of precursor solubility and (ii) increase of diffusion coefficient and decrease of viscosity [12]. The solubility of  $\text{TeO}_2$  increases exponentially with raising temperature and at pH 4.5 a 20- fold increase of solubility from room temperature to 99°C was estimated by Cheng et al [13]. Due to the increase in solubility of  $\text{TeO}_2$  with bath temperature, higher thicknesses were obtained for films deposited at higher bath temperature such as 65°C. It could be observed from Fig. 1 that maximum value of film thickness was obtained from a single deposition within 60 minutes for all bath temperatures from 35 to 65°C. Further, at lower pH ( $3.0 \pm 0.1$ ), free tellurium was deposited alone and at comparatively higher pH ( $4.0 \pm 0.1$ ), the solution became cloudy due to the precipitation of  $\text{TeO}_2$ . Increasing the tellurium ion concentration in the solution by adding  $\text{TeO}_2$  is limited by the solubility of  $\text{TeO}_2$  at given pH and temperature [14]. Since, tellurium is less electropositive than copper, indium, Te could be more likely to deposit as the element from its ions in an electrolytic bath than Cu and In from its ions. Hence, very low concentration of Te in the electrolytic bath must be maintained when compared to Cu and In ions.

### 3.2. Structural studies

X-ray diffraction patterns were taken out in order to identify crystallinity and phases of the deposited films. From x-ray diffraction data, the interplanar spacing  $d_{hkl}$  was calculated using the Bragg's relation [15]

$$d_{hkl} = n\lambda / 2 \sin\theta \quad (1)$$

The lattice constant of cubic  $\text{CuInTe}_2$  cell was calculated using the relation

$$1/d^2 = h^2 + k^2 + l^2/a^2 \quad (2)$$

where  $\lambda$  is the wavelength of the x-rays used,  $d$  the interplanar spacing,  $n$  the order number. The factor  $d$  is related to  $(hkl)$  indices of the plane and the dimension of the unit cell.

From x-ray diffraction profiles, the crystallite size of the films was calculated using FWHM data and Debye-Scherrer formula

[9,16].

$$D = 0.9\lambda / \beta \cos \theta_B \quad (3)$$

where  $\lambda$  is wavelength of x-rays used ( $\lambda = 1.5418 \text{ \AA}$ ),  $\beta$  is Full Width at Half Maximum of the peak in radians,  $\theta_B$  is Bragg's diffraction angle at peak position in degrees.

The strain  $\epsilon$  was calculated from the slope of  $\beta \cos \theta$  versus  $\sin \theta$  plot using the relation [16]

$$\beta = [\lambda / D \cos \theta] - [\epsilon \tan \theta] \quad (4)$$

The dislocation density is defined as the length of dislocation lines per unit volume of the crystal (Williamson and Smallman) [17]. The dislocation density is given by

$$\delta = 1/D^2 \quad (5)$$

The stacking fault probability  $\alpha$  is the fraction of layers undergoing stacking sequence faults in a given crystal and hence one fault is expected to be found in  $1/\alpha$  layers. The presence of stacking sequence fault in peak position of different reflections with respect to ideal positions of a fault-free well annealed powder sample. A well annealed powder sample reference is used to compare the shift in the peak position of different reflections and hence to evaluate the stacking fault probability. The relation connecting stacking fault probability ( $\alpha$ ) with peak shift  $\Delta(2\theta)$  was given by Warren and Warekoi [18]. The stacking fault probability  $\alpha$  is given by

$$\alpha = [2\pi^2/45\sqrt{3}] [\Delta(2\theta)/\tan\theta] \quad (6)$$

From the above expression (6) stacking fault probability was calculated for CuInTe<sub>2</sub> thin films.

### 3.2.1. Effect of bath temperature on structural properties

X-ray diffraction patterns recorded for the electrodeposited CuInTe<sub>2</sub> thin films on ITO substrates with bath composition of 0.001 M CuSO<sub>4</sub>, 0.005 M In<sub>2</sub>(SO<sub>4</sub>)<sub>3</sub> and 0.0005 M TeO<sub>2</sub> are shown in Fig. 2.a,b,c,d. The observed diffraction peaks of CuInTe<sub>2</sub> are found at  $2\theta$  values of angles 25.31, 29.33, 41.96, 49.65, 52.04, 60.86, 68.98, 76.70 corresponding to the lattice planes (111), (200), (220), (311), (222), (400), (420) and (422), respectively. XRD studies revealed that the films of CuInTe<sub>2</sub> are polycrystalline in nature with cubic structure with lattice constant ( $a = 6.080 \text{ \AA}$ ). The different peaks in the diffractogram were indexed and the corresponding values of interplanar spacing "d" were calculated and compared with standard JCPDS values [19]. It is observed from Fig. 2 that the films deposited at bath temperature above 50°C are found to be poorly crystallized and the films deposited above 50°C are found to be well crystallized with preferential orientation along (200) plane. It is also observed from Fig. 2 that the height of the preferential peak increases and some new peaks of CuInTe<sub>2</sub> begins to appear while increasing bath temperature from 35 to 65°C, thereafter the height of the preferential peak slightly decreases. Hence, the bath temperature is fixed as 65°C for all depositions. The films deposited at 65°C have good crystallinity and well adherent to the substrates. Similar behaviour is noted for ZnHgTe thin films reported earlier [15].

### 3.2.2. Effect of deposition potential on structural properties

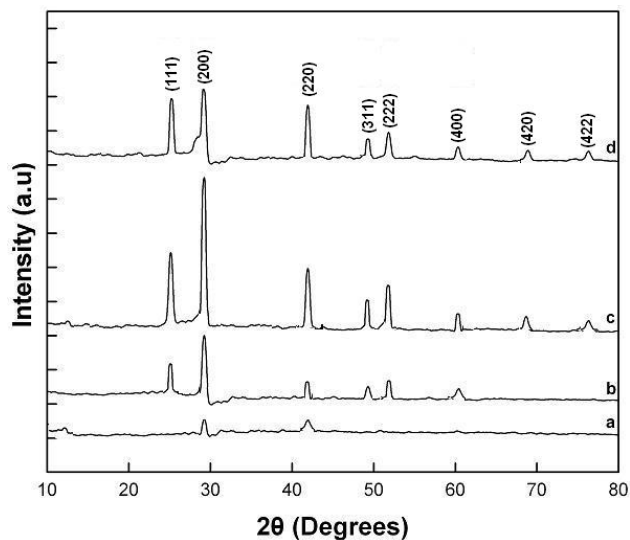


Figure 2. X-ray diffraction patterns of CuInTe<sub>2</sub> thin films electro-deposited at various bath temperatures (a) 35°C (b) 50°C, (c) 65°C, (d) 80°C.

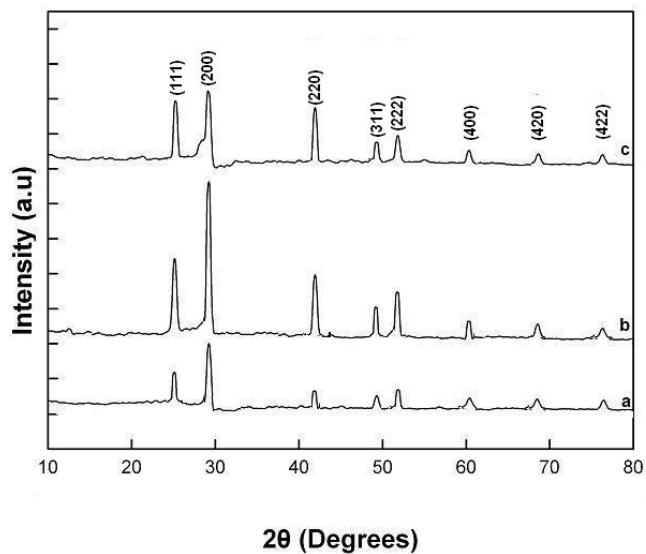


Figure 3. X-ray diffraction patterns of CuInTe<sub>2</sub> thin films electro-deposited at different deposition potentials (a) -700, (b) -900, (c) -1100 mV versus SCE.

X-ray diffraction patterns recorded for electrodeposited CuInTe<sub>2</sub> thin films on ITO substrates with electrolyte concentration of 0.001 M CuSO<sub>4</sub>, 0.005 M In<sub>2</sub>(SO<sub>4</sub>)<sub>3</sub> and 0.0005 M TeO<sub>2</sub> prepared at different deposition potentials is shown in Fig. 3.a,b,c. X-ray diffraction results revealed that the films prepared at different deposition potentials exhibit cubic structure with a preferential orientation along (200) plane. All the peak intensities are found to increase when the deposition potential decreased down to -700 mV versus SCE indicating the polycrystalline morphology of good quality films. The stoichiometric films of good quality are obtained at a deposition potential closer to -900 mV versus SCE. This study

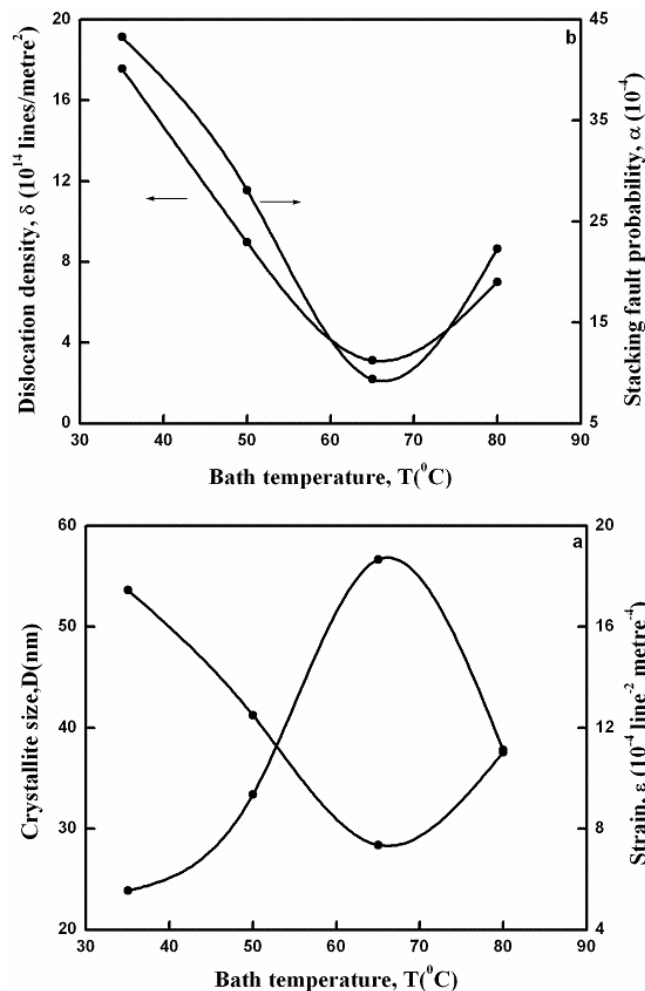


Figure 4. Variation of (a) Crystallite size and Strain, (b) Dislocation density and Stacking fault probability with bath temperature for CuInTe<sub>2</sub> thin films.

shows that the deposition potential does not change the structural phase of CuInTe<sub>2</sub> thin films. However, an increase in crystallinity of the films with deposition potential upto -1100 mV versus SCE is indicated. Hence, the deposition potential is fixed as -900 mV versus SCE used to deposit CuInTe<sub>2</sub> thin films. Similar behaviour is noted for FeSe<sub>2</sub> thin films reported earlier [20].

### 3.2.3. Effects of bath temperature and deposition potential on microstructural parameters

X-ray diffraction pattern of CuInTe<sub>2</sub> thin films prepared at various bath temperatures between 35 and 80°C are recorded. Using FWHM data and Debye-Scherrer formula, the crystallite size of the films were calculated. The strain  $\epsilon$  was calculated from the slope of  $\beta \cos \theta$  versus  $\sin \theta$  plot using equation (4). The variation of crystallite size, strain with bath temperature for CuInTe<sub>2</sub> thin films deposited at 35, 50, 65, 80°C is as shown in Fig. 4a. It is observed from Fig. 4a that the crystallite size increases with bath temperature and the films deposited at 65°C are found to have maximum value of crystallite size. Due to the removal of defects in the lattice with increase in bath temperature the strain in the film gets released and attained a minimum value at 65°C. Using equation (5) and (6) the

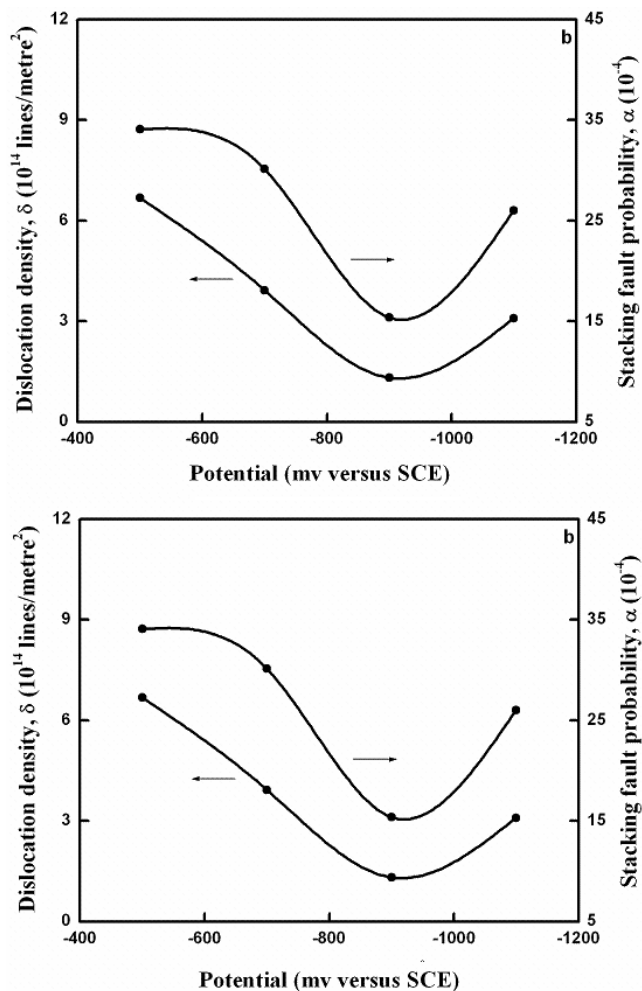


Figure 5. Variation of (a) Crystallite size and Strain, (b) Dislocation density and Stacking fault probability with deposition potential for CuInTe<sub>2</sub> thin films.

dislocation density and stacking fault probability were calculated. The variation of dislocation density and stacking fault probability with bath temperature for CuInTe<sub>2</sub> thin films is shown in Fig. 4b. It is observed from Fig. 4b that both dislocation density and stacking fault probability are found to decrease while increasing bath temperature from 35°C to 65°C, thereafter both of them are slightly increases. A sharp increase in crystallite size and decrease in strain with bath temperature is indicated in Fig. 4a. Such a release in strain reduced the variation of interplanar spacing thus leads to decrease in stacking fault probability and dislocation density of CuInTe<sub>2</sub> thin films and minimum values are obtained for films deposited at 65°C. CuInTe<sub>2</sub> thin film with lower strain, dislocation density and stacking fault probability improves the stoichiometry of the films which in turn causes the volumetric expansion of thin films. Crystallinity improvement with bath temperature enhances the concentration and mobility of Cu, In ion vacancies within the lattice and hence reduces the resistivity of the deposited films. The studies on functional dependency of microstructural parameters on bath temperature indicates that the strain, dislocation density and stacking fault probability decreases with bath temperature whereas

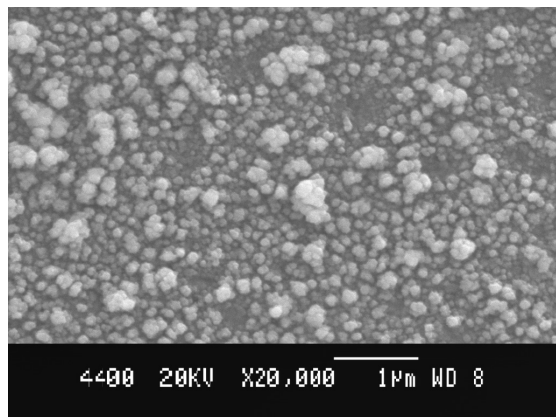


Figure 6. SEM picture of  $\text{CuInTe}_2$  thin films deposited at bath temperature  $65^\circ\text{C}$  and at a deposition potential  $-900$  mV versus SCE.

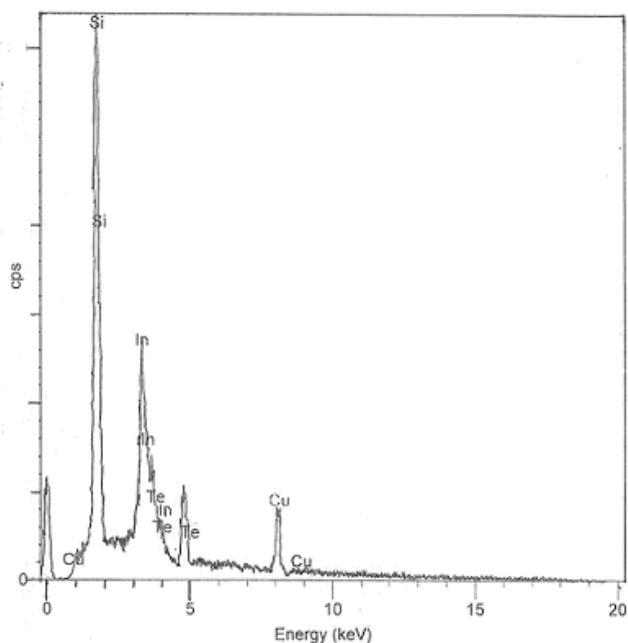


Figure 7. EDAX spectrum of  $\text{CuInTe}_2$  thin film deposited at bath temperature of  $65^\circ\text{C}$  and at deposition potential of  $-900$  mV versus SCE.

the crystallite size increases. Similar functional dependency of microstructural parameters with bath temperature for  $\text{FeSe}_2$  thin films have been reported earlier [10].

The variation of crystallite size, strain with respect to deposition potential was studied and shown in Fig. 5a. It is observed from Fig. 5a the maximum value of crystallite size, minimum value of strain, dislocation density and stacking fault probability are noted for films obtained at a deposition potential of  $-900$  mV versus SCE. Fig. 5b shows the variation of dislocation density and stacking fault probability with deposition potential for  $\text{CuInTe}_2$  thin films. It is observed from Fig. 5b that both dislocation density and stacking fault probability are found to decrease while decreasing deposition potential to  $-900$  mV versus SCE, thereafter both of them are

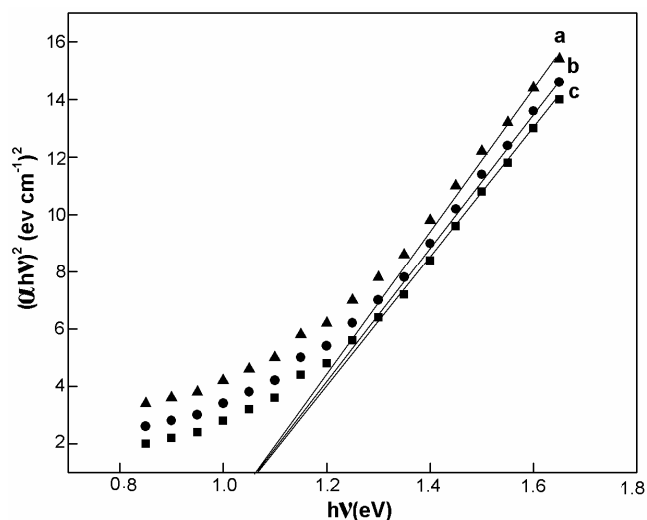


Figure 8.  $(\alpha h\nu)^2$  versus  $h\nu$  plot for  $\text{CuInTe}_2$  thin film electrodeposited at various bath temperatures (a)  $35^\circ\text{C}$ , (b)  $50^\circ\text{C}$  (c)  $65^\circ\text{C}$ .

slightly increases. X-ray diffraction and deposition kinetic studies showed the formation of  $\text{CuInTe}_2$  films with larger crystallite size at a deposition potential  $-900$  mV versus SCE. It is observed from above Fig. 5.a,b, that the strain, dislocation density, stacking fault probability are decreased while decreasing deposition potential, whereas the crystallite size increases. Similar behaviour is noted for  $\text{FeSe}$  thin films reported earlier [9].

### 3.3. Morphological and compositional analyses

The surface morphology of  $\text{CuInTe}_2$  thin film electrodeposited at bath temperature  $65^\circ\text{C}$  and at a deposition potential  $-900$  mV versus SCE is shown in Fig. 6. The surface is observed to be smooth, uniform and covered with spherically shaped grains. The grains are distributed uniformly over the entire surface of the films. The grains are visible in the SEM picture thus represent aggregates of very many small crystallites. Several smaller crystallites are grouped together to form a larger grain. The sizes of the grains are found to be in the range between  $0.14$  and  $0.62$   $\mu\text{m}$ . The average sizes of the grains are found to be  $0.36$   $\mu\text{m}$ .

The film composition was analyzed using EDAX microanalytic unit attached with SEM. A typical EDAX spectrum of  $\text{CuInTe}_2$  thin film coated on ITO substrate at bath temperature  $65^\circ\text{C}$  and at a deposition potential  $-900$  mV versus SCE is shown in Fig. 7. It is observed from Fig. 7 that the emission lines of Cu, In and Te was present in the investigated energy range indicates the formation of  $\text{CuInTe}_2$  thin films. The atomic percentage of  $\text{CuInTe}_2$  thin film deposited at bath temperature  $65^\circ\text{C}$  and at a deposition potential  $-900$  mV versus SCE was found to be  $26.72$  % for Cu,  $28.61$  % for In and  $44.67$  % for Te. The atomic molar ratio of Cu:In:Te was found to be  $1:1.03:1.67$ . This result is consistent with x-ray diffraction analysis of the sample with phase corresponding to  $\text{CuInTe}_2$ . Therefore the film deposited at bath temperature  $65^\circ\text{C}$  and at a deposition potential  $-900$  mV versus SCE are nearly stoichiometric. This result is in agreement with the result reported earlier [1].

### 3.4. Optical properties

Optical transmission spectra of electrodeposited  $\text{CuInTe}_2$  thin

films were recorded as a function of wavelength in the range between 300 and 1200 nm. Substrate absorption, if any was corrected by introducing an uncoated ITO substrate in the reference beam. The absorption coefficient rises sharply owing to the band-to-band transitions, and levels off later. The nature of transition is determined from the absorption coefficient using from the following relation [9]

$$\alpha h\nu = A (h\nu - E_g)^n$$

where A is a constant (slope) and  $E_g$  is the energy gap,  $n=1/2$  for allowed direct transition and  $n=2$  for allowed indirect transition. From the calculated values of the absorption coefficient a plot of  $(\alpha h\nu)^2$  against  $h\nu$  is drawn for films obtained at various bath temperatures and the linear portion of the graph is extrapolated to the energy axis as shown in Fig. 8. The intersection point gives the direct band gap energy of the material and is found to be 1.04 eV. It is found that the band gap value of the samples obtained in the present work is closer to the value reported earlier [3].

#### 4. CONCLUSIONS

Thin films of  $\text{CuInTe}_2$  were deposited on indium doped tin oxide coated conducting glass substrates at various bath temperatures and deposition potentials using an electrodeposition technique. Structural studies shows that the deposited films possess cubic structure with preferential orientation along (200) plane. The microstructural parameters such as crystallite size, strain, dislocation density and stacking fault probability were evaluated and are found to depend upon the deposition conditions. The optimized condition to yield larger crystallite size, lower strain, dislocation density and stacking fault probability are obtained. The surface morphology reveals spherically shaped grains with smooth surface for films deposited at 65°C. Optical transmission measurements indicates that the deposited films has a direct band gap of 1.04 eV which in turn confirms the better crystallinity of  $\text{CuInTe}_2$  thin films. The band gap value of  $\text{CuInTe}_2$  thin films obtained in this work is quite closer to the value reported earlier.

#### 5. ACKNOWLEDGEMENT

One of the authors (S.Thanikaikarasan) is highly thanks to Council of Scientific and Industrial Research (CSIR), New Delhi for the award of Senior Research Fellowship (SRF) to carry out this research work.

#### 6. REFERENCES

- [1] T. Ishizaki, N. Saito, A. Fuwa; Surface and Coatings Technology. 182 (2004) 156.
- [2] J.L. Shay, J.H. Wernick  
Ternary Chalcopyrite Semiconductors: Growth, Electronic Properties and Applications. Pergamon, New York, 1975.
- [3] G. Marin, S.M. Wasim, G. Sánchez Pérez, P.Bocaranda and A.E.Mora; Journal of Electronic Materials. 27 (1998) 1351.
- [4] A.M.Martinez, A.M.Fernández, L.G.Arriaga, U.Cano; Materials Chemistry and Physics. 95 (2006) 270.
- [5] S.Roy, B.Bhattacharjee, S.N.Kundu, S.Chaudhuri, A.K.Pal; Materials Chemistry and Physics. 77 (2002) 365.
- [6] C.Quiroga, R.Oentrich, I.Bonald, E.Medina, D.S.M. Wasin, G. Marin; Physica E. 18 (2003) 292.

- [7] H.P. Wang, W.W. Lam, I. Shih; Journal of Crystal Growth. 200 (1999) 137.
- [8] M.Boustani, K. El Assali, T. Bekkay, A. Khiara; Solar Energy Materials and Solar Cells.45 (1997) 369.
- [9] S.Thanikaikarasan, T.Mahalingam, M.Raja, Taekyu Kim, Yong Deak Kim; Journal of Materials Science:Materials in Electronics (In Press).
- [10]T.Mahalingam, S.Thanikaikarasan, R.Chandramohan, M.Raja, C.Sanjeeviraja, Jong-Ho Kim, Yong Deak Kim; Materials Chemistry and Physics. 106 (2007) 369.
- [11]J.L.Orts, R.Diaz, P.Herrasti, F. Rueda, E. Fatás; Solar Energy Materials and Solar Cells. 91 (2007) 521.
- [12]T.Mahalingam, V.S.John, S.Rajendran and P.J.Sebastian; Semiconductor Science and Technology. 17 (2002) 465.
- [13]K.L.Cheng; Analytical Chemistry. 33 (761) 1961.
- [14]M.Pourbaix; Atlas of Electrochemical Equilibria Aqueous Solutions, Pergamon, New York (1966).
- [15]T.Mahalingam, A.Kathalingam, S.Velumani, Soonil Lee, Hosun Moon and Yong Deak Kim; Journal of New Materials for Electrochemical Systems. 10 (2007) 21.
- [16]S.Velumani, Sa.K.Narayandoss and D.Mangalaraj; Semicond.Sci.Technol. 13 (1998) 1016.
- [17]G.Williamson, R.E. Smallman; Phil. Mag. 1 (1956) 34.
- [18]B.E.Warren, E.P. Warekois; Acta Metall.3 (1955) 473.
- [19]JCPDS Powder Diffraction File Search Manual,89-2930,2003.